



Impacts of *Rhizobium* inoculation and Fe₃O₄ nanoparticles on common beans plants: a magnetic study of absorption, translocation, and accumulation processes

E. Govea-Alcaide · A. DeSouza · E. Gómez-Padilla · S. H. Masunaga ·
F. B. Effenberger · L. M. Rossi · R. López-Sánchez · R. F. Jardim

Received: 8 May 2024 / Accepted: 13 September 2024 / Published online: 30 September 2024
© The Author(s), under exclusive licence to Springer Nature B.V. 2024

Abstract We have carried out a systematic investigation on the impact of Fe₃O₄ nanoparticles (NPs) and *Rhizobium* inoculation on nodulation and growth of common bean plants (cv. Red Guama, *Phaseolus vulgaris*). Three distinct treatments were conducted on the common bean plants: (i) exposure to Fe₃O₄ NPs; (ii) *Rhizobium* inoculation; and (iii) a combined treatment involving Fe₃O₄ NPs + *Rhizobium* inoculation, with non-treated plants as controls. Temperature and magnetic field dependence of magnetization, M(T, H), measurements were performed on both the soil, and dried organs of the plants including roots, nodules, stems, and leaves. M(T, H) analyses indicated a systematic increase in magnetization across organs of plants treated with Fe₃O₄ NPs and combined Fe₃O₄ NPs + *Rhizobium*. We have found the magnetic contribution, generally related to Fe content

in the soil and plant organs, significantly increased in plants exposed to Fe₃O₄ NPs, further indicating absorption, translocation, and accumulation of Fe₃O₄ NPs in the areal parts of the plants. Plants treated with Fe₃O₄ NPs and combined Fe₃O₄ NPs + *Rhizobium* exhibited Fe₃O₄ NPs accumulation in all organs with increasing concentrations of 69.7 to 74.1 N_{NPs}/g in roots, 5.6 to 7.7 N_{NPs}/g in stems, and 3.1 to 5.5 N_{NPs}/g in leaves, respectively. The iron concentration in nodules was found to be close to 65 N_{NPs}/g. No appreciable difference in the absorption index AI of roots between plants treated with Fe₃O₄ NPs (~1.73%) and Fe₃O₄ NPs + *Rhizobium* (~1.79%) has been observed. The translocation index TI increased by ~46% in plants treated with Fe₃O₄ NPs + *Rhizobium* (6.9%) compared to Fe₃O₄ NPs (4.3%). Treated plants showed improved symbiotic performance

E. Govea-Alcaide (✉)
Department of Physics, Federal University of Maranhão,
São Luís, MA 65080-040, Brazil
e-mail: ernesto.govea@ufma.br

E. Govea-Alcaide · A. DeSouza
Department of Physics and Mathematics, Granma
University, Apartado 21, CP 85149 Bayamo, Granma,
Cuba

E. Gómez-Padilla
Facultad de Ciencias Agronómicas, Universidad
Autónoma de Chiapas, Campus V. Km. 87 Carretera
Tuxtla Gutiérrez- Villaflores, C.P. 30470 Villaflores,
Chiapas, México

S. H. Masunaga
Departamento de Física, Centro Universitário FEI, S. B.
Campo, São Paulo, Brazil

S. H. Masunaga · R. F. Jardim
Instituto de Física, Universidade de São Paulo, Rua do
Matão, 1371, São Paulo, SP 05508-090, Brazil

F. B. Effenberger
Instituto de Pesquisas Energéticas e Nucleares, IPEN-
CNEN/SP, São Paulo, SP 05508 000, Brazil

L. M. Rossi · R. López-Sánchez
Instituto de Química, Universidade de São Paulo,
São Paulo, SP, Brazil

including nodule leghaemoglobin and iron content, number of active nodules per plant, and nodule dry weight. The best result was obtained using the combined treatment of Fe_3O_4 NPs + *Rhizobium*. This study provides evidence that M(T,H) measurements constitute a valuable tool in monitoring the uptake, translocation, and accumulation of Fe_3O_4 NPs in plant organs of common bean plants.

Keywords Magnetic measurements · Common bean (*Phaseolus*) · Fe_3O_4 nanoparticles · *Rhizobium* inoculation

Introduction

The application of nanoparticles (NPs) in agriculture is an expanding field of investigation with potential to revolutionize methodologies employed in food cultivation. Nanoparticles, extremely small particles ranging from 1 to 100 nm (nm), find application in various aspects of agriculture. They can enhance nutrient delivery, serving as carriers to transport essential nutrients directly to plant cells, thereby optimizing absorption [72, 74]. Additionally, certain NPs exhibit antimicrobial properties, offering a potential avenue for pest and pathogen control. For example, silver NPs have demonstrated antibacterial and antifungal activities [4, 16, 30, 34, 45, 47]. Moreover, NPs may contribute to soil quality improvement by enhancing structure and water retention, particularly beneficial in regions facing water scarcity [6, 18, 23, 38]. Some NPs, particularly at lower doses, accelerate the production of secondary metabolites, boost the functions of antioxidant enzymes, improve the efficiency of water and fertilizer absorption, and facilitate photosynthesis. These cumulative effects ultimately lead to the promotion of plant growth [32, 37, 60, 69, 72, 76]. Among all types of NPs, iron oxide NPs such as magnetite (Fe_3O_4), hematite ($\alpha\text{-Fe}_2\text{O}_3$), and maghemite ($\gamma\text{-Fe}_2\text{O}_3$) are promising NPs for practical applications due to their great biocompatibility and catalytic, magnetic, antioxidant, anti-microbial, and optical properties [42, 64, 44] being the basis of innovative technologies in the field of science, engineering, and technology.

Fe_3O_4 nanoparticles have attracted increased attention relative to other iron oxides owing to their unique and desirable general magnetic and electronic

properties such as their superparamagnetic behavior, biological compatibility, and low toxicity [50]. The use of Fe_3O_4 NPs offers a broad spectrum of opportunities in the branches of plant research and agronomy [25]. Several investigations have explored the impact of iron oxide nanoparticles on seed germination and the subsequent growth of plants. For instance, it has been observed that daily additions of magnetite nanoparticles and exposure of plants to static magnetic fields resulted in an increase of the growth of *Zea mays* and leaf chlorophyll content [53]. Increased chlorophyll content has also been found in soybean seedlings treated with 9 nm diameter Fe_3O_4 NPs applied at a concentration based on the iron quantity needed for plant growth, with no observed toxicity despite translocation of NPs into soybean stems [22]. Moreover, aqueous suspensions of Fe_3O_4 NPs have been shown to be responsible for the translocation of the magnetic material throughout pumpkin plant tissues and its accumulation in roots and leaves [77]. Significant positive effects of Fe_3O_4 NPs on the plant growth characteristics of wheat have also been found [31]. A progressive and systematic increase in the magnetization signal has been observed in roots, stems, and leaves of common bean plants cultivated in soil treated with increasing concentrations of Fe_3O_4 nanoparticles suspensions [24]. The study indicated that Fe_3O_4 NPs being made available in the soil can be absorbed by the roots, translocated to the aerial parts, and stored in various plant organs. Furthermore, the presence of Fe_3O_4 NPs demonstrated significant positive impact on the chemical characteristics of the soil rhizosphere and the accumulation of nutrients in common bean plants cultivated in such conditions [14].

The mobility of the magnetic nanoparticles (NPs) in the soil, their translocation from soil to plant organs, and their distribution within various plant tissues are crucial factors influencing the impact of magnetic NPs on plant growth [63]. Hence, a comprehensive understanding of the displacement of magnetic NPs in the soil and their internal dynamics within plant organs is essential for accurately predicting the effects of NPs on plant growth [10] and the resulting biochemical, morphological, molecular, and physiological alterations in crops [35]. The mobility of nanoparticles relies on the physicochemical characteristics of both the NPs and their surrounding environment. Magnetic NPs in the

soil surrounding plant roots have the potential to be absorbed by the roots and transported to the aerial parts of plants, including leaves and other above-ground structures, thereby directly influencing their growth [43, 24, 1, 36]. However, direct evidence of NPs transport within plants remains limited [55, 3, 59, 67, 68, 68]. Consequently, it is imperative to investigate the movement and localization of magnetic NPs within various plant structures, including cellular organelles, using magnetic tracking to understand the processes of absorption, translocation, and accumulation of Fe_3O_4 NPs. This is due to the unique magnetic properties of these NPs, such as superparamagnetic or ferrimagnetic behavior [50]. A thorough comprehension of the uptake and transport dynamics of NPs in plants is essential for the optimal design of NPs for agricultural applications [26].

On the other hand, nitrogen fixation, occurring after photosynthesis, is undeniably one of the most vital biologically-mediated processes in plants [70]. This is because all living organisms require nitrogen to create amino acids for protein synthesis. The predominant origin of biologically-fixed nitrogen stems from the symbiotic association between rhizobia and legumes, leading to the development of specialized organs known as nodules [17, 58]. These nodules, found in roots or occasionally in stems, facilitate the conversion of atmospheric nitrogen (N_2) into other forms (ammonium, nitrates, and ammonia) readily assimilated by plants [17, 28, 52]. The efficiency of nitrogen fixation in legumes is contingent on the effective formation of nodules by *Rhizobium*. Inoculating legume seeds can ensure the presence of efficient *Rhizobium* in sufficient quantities in the root environment, enhancing nitrogen fixation upon nodule formation [13, 61]. However, the efficacy of *Rhizobium* inoculation varies based on factors such as host genotype, *Rhizobium* strain efficiency, soil conditions, and climatic factors [51, 41, 49].

The common bean (*Phaseolus vulgaris* L.), considered the most important grain legume [33], is often deemed a relatively inefficient nitrogen fixer [73, 2, 54]. Therefore, exploring the potential benefits of Fe_3O_4 NPs in enhancing its response to

Rhizobium inoculation is a subject that has received limited attention. Recently, the use of Fe_3O_4 NPs, *Rhizobium* inoculation, and their combined application in common bean grown in soil was reported [15, 19]. The results indicated a significant increase of symbiotic performance and nodulation in plants. The treatments led to a remarkable increase in the number of nodules per plant, active nodules per plant, and nodule dry weight. Moreover, they contributed to improve the symbiotic nitrogen fixation, a feature related to the evident through heightened nitrogenase activity, leghemoglobin, and iron contents, as well as increased shoot and root nitrogen content and the quantity of root-fixed nitrogen. The enhanced nodulation and nitrogen fixation positively impacted the overall growth and dry matter production, as indicated by longer roots and shoot lengths, greater leaves area per plant, and increased roots, stems, and leaves dry weights in treated plants. Our findings provided compelling evidence supporting the notion that the presence of Fe_3O_4 NPs in nodules enhances the symbiotic performance between *Rhizobium* (leguminosarum CF1 strain) and common bean plants, positively impacting nodulation and nitrogen fixation.

In this study, an investigation of the influence of Fe_3O_4 NPs, *Rhizobium* inoculation, and their combined application in common beans grown in soil under controlled growth chamber conditions is presented. The main objective was to conduct a systematic study of the absorption, translocation, and accumulation process of Fe_3O_4 NPs through magnetization measurements as a function of temperature, $M(T)$, and applied magnetic field, $M(H)$, by using a Quantum Design SQUID magnetometer. A collection of magnetization data, encompassing $M(T)$ and $M(H)$ measurements, conducted across a wide temperature range from 5 to 300 K and under magnetic fields reaching up to ± 70 kOe is discussed. The recorded magnetic signals in roots, stems, and leaves indicated the absorption of magnetite NPs by common bean plants from the soil, followed by their subsequent accumulation in various plant organs. Additionally, we have found that the symbiotic combination of Fe_3O_4 NPs and *Rhizobium* inoculation has a marked influence on the translocation process from roots to the aerial part of the plants.

Experimental procedure

Seed selection, soil and sowing conditions

Bean seeds certified as genetically similar (*Phaseolus vulgaris* L. cv. Red Guama) were sourced from the Seed Laboratory of the Ministry of Agriculture in Granma Province, Cuba. The selected seeds were free of visible defects, insect damage or malformation, and were carefully stored in desiccators containing 70% (v/v) glycerin. The moisture content of the seeds was 10–12% based on fresh weight before the treatments, and they exhibited a final germination percentage of 90%.

The seeds were planted in a soil mixture that was placed in open polyethylene bags, identified as B0, BH0, BN2, and BH2 (see Table 1), and replicated three times. The soil in these bags had a loamy texture and a pH value of 7.0, classified as brown carbonate. Its composition included 3.2% organic matter, 0.102 gkg⁻¹ assimilable phosphorus, and 0.815 gkg⁻¹ potassium, with a cation exchange capacity (CEC)

of 42.2 meq/100 g, and a base exchange capacity of 31.8 meq/100 g. Furthermore, the soil contained 1.71 gkg⁻¹ Ca, 1.75 gkg⁻¹ K, and 0.530 gkg⁻¹ Mg, while the total nitrogen content was low at 0.75 gkg⁻¹. Based on soil analysis, the nutrients were sufficient for the growth of common bean plants [29]. All the plants were grown in a Conviron growth chamber under controlled conditions, as reported elsewhere [15].

The treatments were administered through morning irrigation starting with 20 mL of water in all bags, *Rhizobium* inoculation in BH0, 20 mL of suspended Fe₃O₄ NPs at a concentration of 2000 mg/L in BN2, and a combination of 20 ml of Fe₃O₄ NPs (2000 mg/L) and *Rhizobium* in BH2. The seeds in bags B0, designated as the control, were grown in soil free of Fe₃O₄ NPs and *Rhizobium* inoculation and received a daily irrigation of 40 mL of water (see Table 1).

The used Fe₃O₄ NPs had a log-normal distribution with a median diameter of 10 nm and a distribution width of 0.36 and were prepared by a coprecipitation

Table 1 Experimental conditions and sample labels

Bag labels	Experimental conditions	Samples labels
B0	Pristine soil	S0
	+	R0
	no <i>Rhizobium</i>	C0
	+	L0
	no Fe ₃ O ₄ NPs	
BH0	+	
	(40 mL H ₂ O)/ day	
	Pristine soil	SH0
	+	RH0
	<i>Rhizobium</i> inoculation *	CH0
BN2	+	LH0
	no Fe ₃ O ₄ NPs	NH0
	+	
	(40 mL H ₂ O)/day	
	Pristine soil	SN2
BH2	+	RN2
	no <i>Rhizobium</i> inoculation	CN2
	+	LN2
	(20 mL of H ₂ O of suspended Fe ₃ O ₄ NPs) / day	
	+	
BH2	(20 mL de H ₂ O)/day	
	Pristine soil	SH2
	+	RH2
	<i>Rhizobium</i> inoculation *	CH2
	+	LH2
BH2	(20 mL of H ₂ O of suspended Fe ₃ O ₄ NPs) / day	NH2
	+	
BH2	(20 mL de H ₂ O)/day	

*See text for inoculation details

method described elsewhere [56]. As mentioned above, to study the effect of Fe_3O_4 NPs, *Rhizobium* inoculation (BHO), and Fe_3O_4 NPs + *Rhizobium* inoculation (BH2) on symbiotic root nodule formation, one seed per bag was inoculated with *Rhizobium leguminosarum* CF1 strain (1 mL of bacterial suspension and 10^8 bacteria mL^{-1} in mannitol) (LM) yeast culture medium, [71] at sowing time and seven 7 days after sowing to induce root nodule formation. Nodules were collected at 28 days post-infection and the number of nodules per plant was determined by counting all nodules on each of the plants and computing the average. The number of active nodules per plant was determined by cutting nodules in each of them and observing their internal color, ranging from pink to reddish. The dry weight of nodules per plant was determined by drying samples at 80°C for 3 days to a constant weight.

Plant growth, sample preparation, and quantitative analysis

Plants were allowed to grow for 35 days after sowing until the establishment of vegetative growth. Then, they were removed from the bags and rinsed well with deionized water to remove excess soil from the roots, and then cut into short pieces. The plant segments were dried at room temperature for 15 days. After this step, each part of the plants was manually ground for about 30 min to form a fine powder for all characterizations. From each polyethylene bag, four samples were separated: soil (S), roots (R), stems (T), and leaves (L). For example, roots extracted from bags B0, BH0, BN2, and BH2 were identified and labeled as samples R0, RH0, RN2, and RH2, respectively. The corresponding labels were applied to soils (S0, SH0, SN2, and SH2), stems (T0, TH0, TN2, and TH2), and leaves (L0, LH0, LN2, and LH2). Nodules from bags BH0 and BH2 were collected and labeled as NH0 and NH2, respectively. A summary of sample labels and specific treatment for each samples are presented in Table 1.

The nodules on each individual root were counted, and those fresh and dry (at 70°C for 48 h) masses were used for all the measurements. Nodules (500 mg) were homogenized in aliquots of Drabkin's reagent (10 ml), and the leghaemoglobin was quantified spectrophotometrically at A540. An analysis of the iron content in each soil and dried plant

sample was conducted by using an inductively coupled plasma optical emission spectrometer (ICP-OES) Spectro Arcos (Spectro) [24].

The data pertaining to active nodules, nodule dry weight, leghaemoglobin content, and total Fe content in soils, nodules, roots, and leaves were subjected to statistical analysis using two-way ANOVA ($P < 0.05$) as reported elsewhere. This analysis aimed to determine the effects of the applied treatments in comparison to the sample control. Mean comparisons were performed using the Newman-Keuls test [62]. The normality of the data was assessed through the Kolmogorov-Smirnov procedure, and homogeneity of variances among treatments was tested using the Bartlett's test [75]. All statistical analyses were conducted using the 'Statistica for Windows' software package, version 10 (StatSoft, Tulsa, UK).

Magnetization measurements

Magnetization measurements were performed in a commercial Quantum Design SQUID magnetometer in powder samples. The magnetization as a function of temperature $M(T)$ was performed under both zero-field cooled (ZFC) and field-cooled (FC) conditions. Also, the magnetic field dependence of the magnetization, $M(H)$, was measured in the magnetic field range $-70 \leq H \leq 70$ kOe, and for selected temperatures of $T = 10$ and 300 K. The magnetization data, denoted as $M(T, H)$, were adjusted to eliminate the inherent magnetic response of the plants. For plants irrigated with Fe_3O_4 NPs and Fe_3O_4 NPs and *Rhizobium*, the reported magnetization data as a function of temperature and applied magnetic field is expressed as:

$$M(T, H) = M_{\text{med}}(T, H) - M_0(T, H), \quad (1)$$

where $M_{\text{med}}(T, H)$ denotes the raw data measured in plants from bags BN2 or BH2, and $M_0(T, H)$ represents the raw data measured in the control plant of bag B0. In the case of nodules, $M_0(T, H)$ is taken as reference for the bag BH0.

Results and discussion

The application of Fe_3O_4 NPs and the combined treatment of Fe_3O_4 NPs and *Rhizobium* exhibited a similar qualitative behavior in all part of the plants.

The Fe content increases abruptly and remains almost constant in the treated plants. Also, its values tend to decrease ~65% from soil to leaves in plants grown in bags BN2 and BH2. However, the observed increase in iron content can be used as an indication of the absorption, translocation, and accumulation of Fe_3O_4 NPs in different part of the plants. As far as this point is concerned, Fig. 1(a) shows the iron concentration in the soil and different organs of the bean plants. Our focus on these parameters is motivated by their relevance to detect the presence of Fe_3O_4 NPs in treated plants (bags BN2 and BH2) compared to the untreated plants (B0 and BH0).

The treatments significantly increased ($P < 0.05$) the number of active nodules per plant by ~30% and the nodule dry weight by ~20% between NH0 and NH2 (Fig. 1(b)). In this regard, a high nodule dry weight is generally associated with the increased nitrogen fixation in legumes, as reported elsewhere [20]. Moreover, after the nodules were collected from roots RH0 (NH0) and RH2 (NH2), respectively, they exhibited pink to dark red coloration, a feature usually attributed to either the presence of leghaemoglobin and a higher number of active nodules in treated plants. Furthermore, as observed in Fig. 1(b), the leghaemoglobin and iron content were observed to increase by ~26 and ~71%, respectively, with the use of combined treatment of Fe_3O_4 NPs and *Rhizobium*. These findings suggest an enhancement in the symbiotic performance between *Rhizobium* and common bean plants in the presence of Fe_3O_4 NPs. The increased number of active nodules implies an expanded area for bacteroids, which is generally associated with the potential for nitrogen fixation [15, 70]. The elevated symbiotic performance and nodulation observed in treatment NH2 stems from the favorable combination of the efficiency of the introduced *Rhizobium* strain, to compete with indigenous bacteria in the soil, and the action of the Fe_3O_4 NPs.

It is important to point out that Leghaemoglobin is crucial in maintaining optimal oxygen (O_2) levels (20–40 nM) for respiration in bacteroid-containing cells of bean root nodules, thereby preventing the inactivation of the nitrogenase enzyme, which is essential for nitrogen (N_2) fixation into ammonia (NH_3). This process supports the production of ATP and ensures the effective functioning of nitrogenase in symbiotic nitrogen fixation [5, 8, 11]. Fe_3O_4 nanoparticles can be absorbed by bean plant roots due to

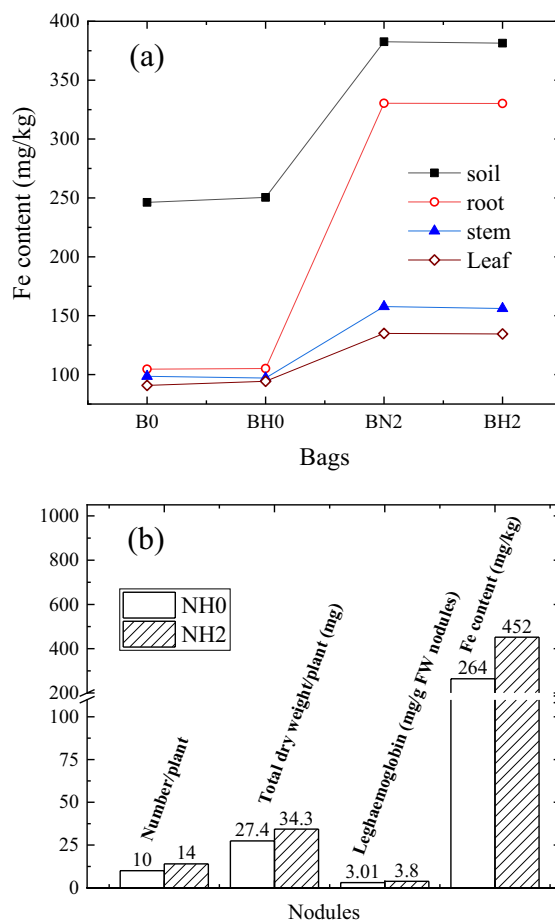


Fig. 1 Parameters extracted from different organs of bean plants and in nodules from bags BH0 and BH2 (Sample labels are listed in Table 1). **a** Iron concentration in different organs of common bean plants. **b** Nodules number per plant, total dry weight of nodules per plant, leghaemoglobin, and Fe content, respectively (see Ref. ([15] for more details)

their positive charge and high surface reactivity [40, 48]. These NPs release iron in the Fe^{2+} form, which binds to leghaemoglobins, facilitating respiration and nodulation in bean plants [39]. The iron released by Fe_3O_4 NPs enhances the oxygen transport capacity of leghaemoglobin and nitrogenase activity, leading to increased nitrogen fixation in nodules [9, 12, 27]. Fe_3O_4 NPs possess properties such as biocompatibility, catalytic efficiency, and superparamagnetism, which help them participate effectively in cellular processes and improve genetic and physiological responses in plants [66].

As mentioned in the introduction, the main focus of this study is to trail the absorption, translocation, and

accumulation processes in common bean plants subjected to both Fe_3O_4 NPs and their interaction with the *Rhizobium* inoculation treatment. This investigation is conducted through magnetization measurements, a technique proven to be effective in detecting and quantifying magnetic NPs in different types of plants [24, 65, 67, 68, 68, 77]. However, for the sake of comparison, it is mandatory to initially assess the magnetic response of isolated Fe_3O_4 NPs. The magnetic properties of Fe_3O_4 NPs used in this work were previously investigated and reported by [24]. The $M(T)$ curves, measured under a magnetic field of 500 Oe, exhibit a blocking temperature (T_B) of approximately 130 K and an irreversibility temperature (T_{ir}) of around 220 K (refer to Fig. 2 in [24]). The saturation magnetization, M_s , at 10 and 300 K were found to be 82.8 and 68.5 emu/g, respectively. At 10 K, the magnetic hysteresis is characterized by a remnant magnetization $M_r \sim 16$ emu/g and a coercivity $H_c \sim 200$ Oe. For $M(H)$ data at 300 K, well above T_B , a small hysteresis was detected with $M_r = 0.9$ emu/g and $H_c \sim 10$ Oe. The mean diameter of Fe_3O_4 NPs, \bar{d} , and its size distribution width were determined by fitting the $M(H)$ data at room temperature to the Langevin function. The reported values were $\bar{d} = 6.7$ nm and $\sigma = 0.4$, respectively, which are closed to that shown in transmission electron microscopy image of these Fe_3O_4 NPs, also reported in the same reference. Thus, our next analysis aims to compare the magnetic response of isolate Fe_3O_4 NPs qualitatively and quantitatively with those measured in soils and different plant organs.

Figure 2 shows the magnetic characterization for the soil taken from bags B0, BH0, BN2, and BH2, respectively. The $M(T)$ signal in the untreated samples S0 and SH0 is almost one order of magnitude smaller than that measured in samples SN2 and SH2, subjected to treatment with Fe_3O_4 NPs (see Fig. 2(a)). The magnetic behaviors of S0 and SH0 yielded to both qualitative and quantitative similarities, that is: they exhibit a clear paramagnetic-like response, implying the absence of Fe_3O_4 NPs in these samples. In contrast, the $M(T)$ data displayed in Fig. 2a for samples SN2 and SH2 resemble the magnetic behavior reported for isolated magnetic Fe_3O_4 NPs used in our experiments [24]. The $M(T)$ curves for SN2 and SH2 display a broad maximum in the ZFC branch of the curves, at $T_B \sim 100$ K in both samples. It is also observed that ZFC curve separates from the FC one at $T_{ir} \sim 160$ and 180 K for SN2 and SH2, respectively.

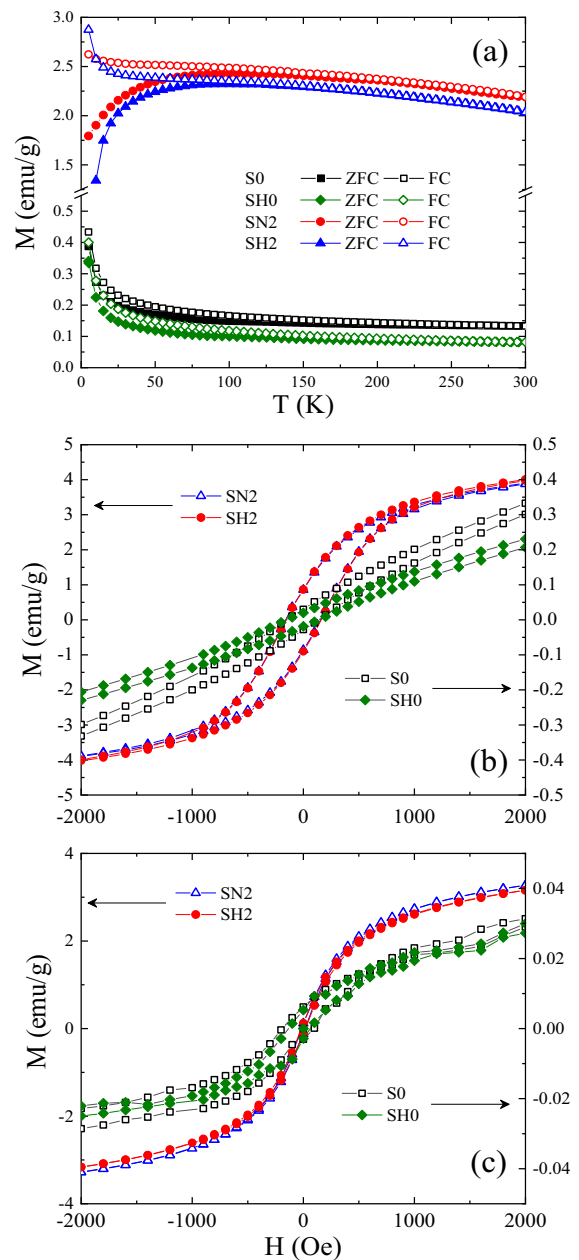


Fig. 2 a Temperature dependence $M(T)$ of magnetization curves under ZFC (closed symbols) and FC (open symbols) conditions in soil samples S0, SH0, SN2, and SH2 (Sample labels are listed in Table 1). b $M(H)$ curves measured at $T = 10$ K. c $M(H)$ curves taken at $T = 300$ K

Figure 2(b) and (c), on the other hand, display the $M(H)$ curves for samples S0, SH0, SN2, and SH2, measured at 10 and 300 K, respectively. The data clearly indicate that $M(H)$ for samples SN2 and SH2,

irrigated with Fe_3O_4 NPs, exhibit higher remanence and coercivity at 10 K compared to room temperature. At 10 K, the values of M_r and H_c were 0.87 emu/g and 150 Oe, while at 300 K, these values were found to decrease appreciably to $4 \cdot 10^{-4}$ emu/g and 20 Oe, respectively. A careful examination of Fig. 2(b) and (c) confirms the similarity of these results in both samples. Consistent with the results of $M(T)$ curves, the $M(H)$ data at 10 and 300 K obtained for untreated samples S0 and SH0, not subjected to the Fe_3O_4 NPs treatment, exhibited only weak paramagnetic behavior, further indicating the absence of magnetic compounds within the samples and, consequently, Fe_3O_4 NPs. This result provides support for the presence of Fe_3O_4 NPs in the soil of plants exposed to Fe_3O_4 NPs and the combined treatment of Fe_3O_4 NPs and *Rhizobium* inoculation.

Figures 3, 4, and 5 show the overall $M(T, H)$ curves for roots, stems, and leaves samples taken from bags B0, BH0, BN2, and BH2, separately. Notably, the $M(T)$ curves displayed in Figs. 3(a), 4(a), and 5(a) for samples R0, RH0, C0, CH0, L0, and LH0 show a paramagnetic-like behavior, a feature like that observed for samples S0 and SH0. Such a similarity is consistent with the absence of magnetic NPs in any organ of the untreated plants. In addition to this, the $M(H)$ curves conducted at both 10 K and 300 K further support the observed behavior in untreated plants (see for instance Figs. 3(b) and (c), 4, and 5(b) and (c)), further adding credence to the absence of Fe_3O_4 NPs in these untreated plant organs.

In contrast, the magnetic responses of samples taken from organs of plants grown in bags BH2 and BN2, treated with Fe_3O_4 NPs, exhibit different features. As far as this point is concerned, Figs. 3, 4, and 5 show $M(T)$ and $M(H)$ data for roots, stems, and leaves extracted from those plants irrigated with Fe_3O_4 NPs and with a combination of Fe_3O_4 NPs + *Rhizobium*. Some relevant parameters extracted from these curves are listed in Table 2. Remarkably, all $M(T)$ curves exhibit a qualitatively similar response to those observed in the treated soils SN2 and SH2 (see Fig. 2(a)). For the organs of the plants grown in bags BH2 and BN2, the blocking temperature T_B was found to be within the range of 90 – 105 K. These values of T_B are very close to those found in samples SN2 and SH2 ($T_B \sim 100$ K) and somewhat lower than those reported for pristine Fe_3O_4 NPs ($T_B \sim 130$ K). These results indicate the

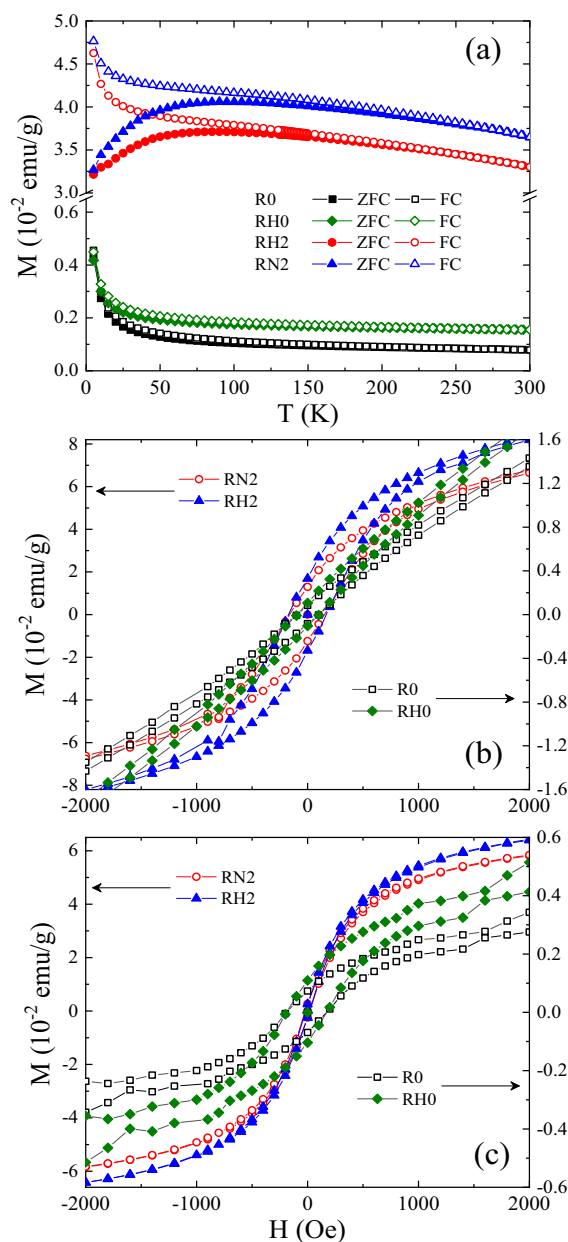


Fig. 3 **a** Temperature dependence $M(T)$ of magnetization curves under ZFC (closed symbols) and FC (open symbols) conditions in roots samples R0, RH0, RN2, and RH2 (Sample labels are listed in Table 1). **b** $M(H)$ curves measured at $T = 10$ K. **c** $M(H)$ curves taken at $T = 300$ K

presence of detectable amounts of Fe_3O_4 NPs in all organs of the treated plants. Furthermore, the quantitative analysis of the $M(T)$ data also suggests a significant and progressive decrease in the content of Fe_3O_4 NPs from roots to leaves.

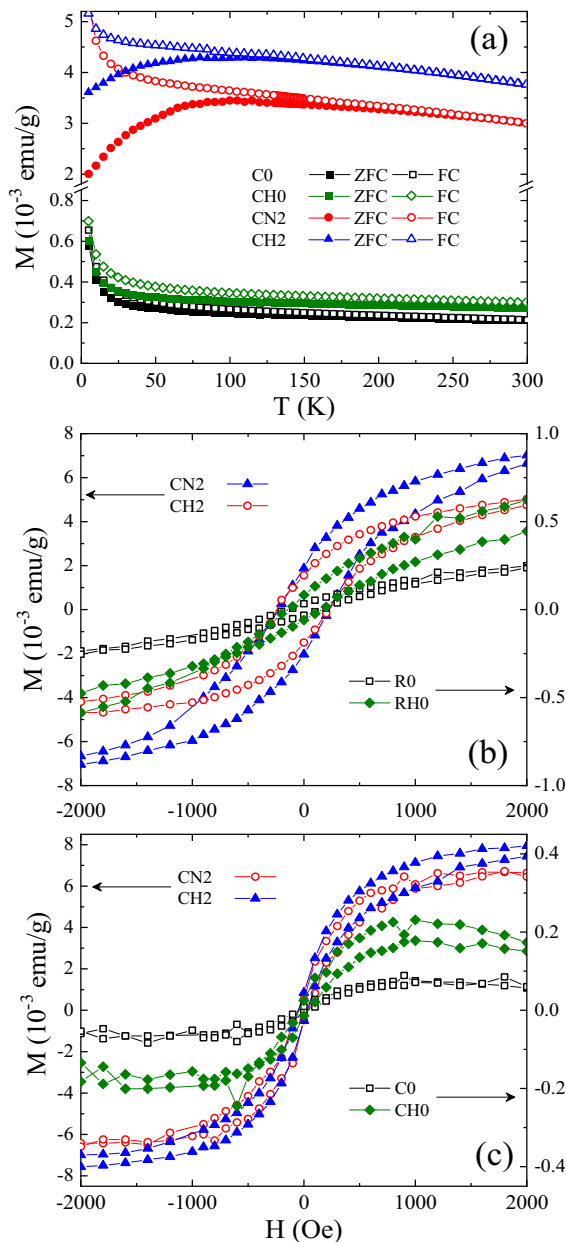


Fig. 4 **a** Temperature dependence $M(T)$ of magnetization curves under ZFC (closed symbols) and FC (open symbols) conditions in stems samples C0, CH0, CN2 and CH2 (Sample labels are listed in Table 1). **b** $M(H)$ curves measured at $T = 10$ K. **c** $M(H)$ curves taken at $T = 300$ K

In addition to the analyses of magnetization data discussed above, it is important to explore some of the other features in greater detail. The $M(H)$ curves for various plant organs, measured at both 10 K and 300 K, exhibit consistent magnetic response.

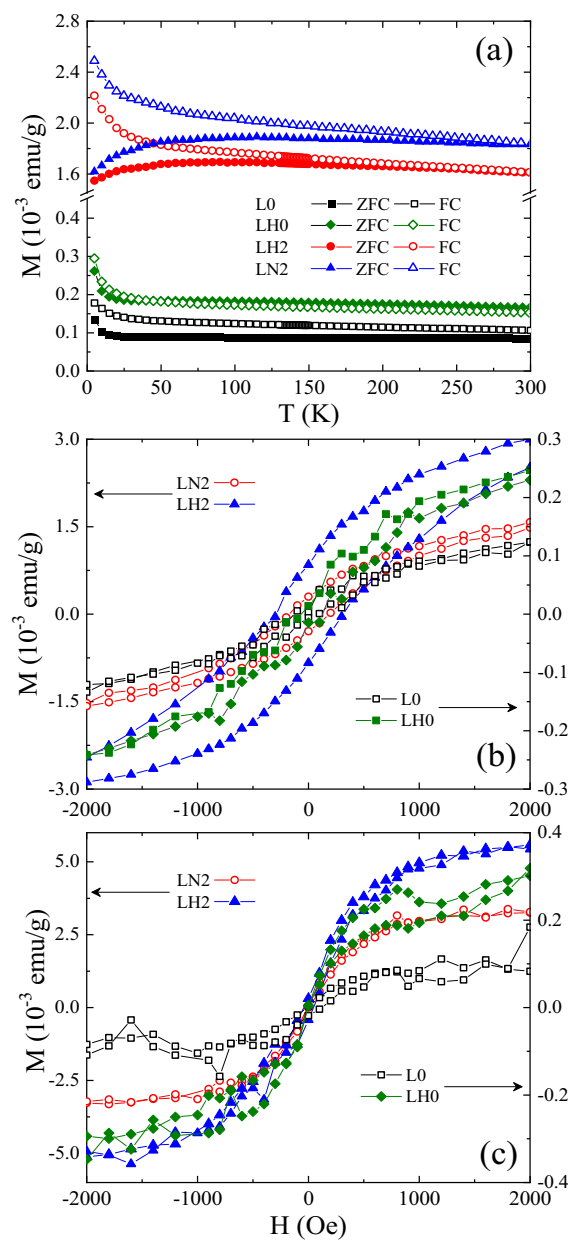


Fig. 5 **a** Temperature dependence $M(T)$ of magnetization curves under ZFC (closed symbols) and FC (open symbols) conditions in leaves samples L0, LH0, LN2, and LH2 (Sample labels are listed in Table 1). **b** $M(H)$ curves measured at $T = 10$ K. **c** $M(H)$ curves taken at $T = 300$ K

Specifically, the $M(H)$ curves for each plant organ, measured at 10 K, or more appropriately for $T \ll T_B$, exhibit a clear magnetic hysteresis, indicating the blocked state of Fe_3O_4 NPs. Values of coercivity for plant organs are in the range 160 – 260 Oe (Table 2).

Table 2 Magnetic parameters of the studied samples extracted from magnetic measurements: T_B is the blocking temperature, M_s is the saturation magnetization measured at 300 K

Samples	T_B (K)	H_c (Oe) 10 K	M_r (10^{-3} emu/g) 10 K	M_s (10^{-3} emu/g) 300 K
SN2	100	155	861	4016
SH2	95	158	86.0	4142
RN2	90	169	16.8	69.7
RH2	90	161	12.9	74.1
CN2	100	230	1.6	5.6
CH2	105	236	1.9	7.7
LN2	95	172	0.3	3.1
LH2	105	260	0.8	5.5
NH2	95	169	16.3	64.5

M_r and H_c are the remanent magnetization and coercivity, respectively, measured at 10 K. Reported values were extracted from data measured in soils (S), roots (R), stems (C), and nodules (N) of bags irrigated with Fe_3O_4 NPs and Fe_3O_4 NPs + *Rhizobium*

In contrast, at 300 K ($T > T_B$), the magnetic hysteresis is very small suggesting that Fe_3O_4 NPs are in a superparamagnetic state. The quantitative investigation of the $M(H)$ curves from the roots to the aerial part of the plants (leaves) reveals significant variations, consistent with the above $M(T)$ findings. For instance, the saturation magnetization, M_s , was found to decrease from $69.7 \cdot 10^{-3}$ ($74.1 \cdot 10^{-3}$) emu/g in samples RN2 (RH2) to $3.1 \cdot 10^{-3}$ ($5.5 \cdot 10^{-3}$) emu/g in LN2 (LH2), respectively.

In our previous investigation, Fe_3O_4 NPs were detected in all plant organs of the treated plants. To move forward at this point, we have defined the number of Fe_3O_4 NPs per mass of dry plant organs, denoted as $N_{NPs} = M_s / \mu_{Fe_3O_4 \text{ NPs}}$, where $\mu_{Fe_3O_4 \text{ NPs}}$ is the magnetic moment of an individual Fe_3O_4 NPs. The N_{NPs} can be then used as an indicator of the number of accumulated NPs in the plant organs [24]. Thus, considering the values of M_s listed in Table 2, lead one to conclude that the treated plants accumulated Fe_3O_4 NPs in all organs. In addition, the observed reduction in M_s indicates a decreasing content of accumulated Fe_3O_4 NPs from roots to leaves. It is noteworthy that the saturation magnetization (M_s) is higher when comparing the same plant organ exposed to different treatments, specifically, Fe_3O_4 NPs and Fe_3O_4 NPs + *Rhizobium* (refer to Table 2). For example, upon comparing the amount

of accumulated NPs between samples LN2 and LH2, an increase of $\sim 77\%$ is evident in the leaves of the plants treated with NPs + *Rhizobium*. This result indicates that *Rhizobium* inoculation plays a crucial role in enhancing the translocation of iron nutrients from the soil to the aerial parts of the plant.

We might recall that the accumulation process of magnetic NPs to the areal organs of the plants is preceded by those of absorption and translocation, respectively. Absorption primarily takes place from soil to roots; for a rough estimation of the absorption index, AI, the relation $AI(\%) = (N_{NPs}^{root} / N_{NPs}^{soil}) \cdot 100 = (M_s^{root} / M_s^{soil}) \cdot 100$ is of interest. From the M_s values listed in Table 2, no appreciable difference in the AI was observed between samples RN2 ($\sim 1.73\%$) and RH2 ($\sim 1.79\%$). On the other hand, the translocation index TI, calculated following the relation $TI(\%) = N_{NPs}^{leaves} / (N_{NPs}^{root} + N_{NPs}^{leaves}) = (M_s^{leaves} / (M_s^{root} + M_s^{leaves})) \times 100$, expresses other relevant indicator to the discussion. It is important to point out that the translocation process was exclusively assessed from roots to leaves (aerial part or shoots). The results here revealed values of 4.3% and 6.9% in samples LN2 and LH2, respectively. It is worth emphasizing that the translocation index was found to increase by $\sim 46\%$ in plants treated with Fe_3O_4 NPs + *Rhizobium* in comparison with the control plants, despite the absence of appreciable difference in the absorption among the treated plant samples. Such an increase of TI strongly indicates that *Rhizobium* inoculation significantly contributes to the enhanced translocation of iron nutrients from the soil to the aerial parts of the plant. To further investigate this point, we will first examine the capability of *Rhizobium* nodules to absorb and accumulate Fe_3O_4 NPs. Therefore, Fig. 6 displays the overall magnetic characterization of samples NH0 (untreated) and NH2 (treated with Fe_3O_4 NPs). For nodules of untreated sample, the magnitude of the magnetic signal is very low, suggesting, as expected, the absence of Fe_3O_4 NPs in the sample. On the contrary, the $M(T)$ and $M(H)$ data acquired at 10 and 300 K closely resemble the behavior observed in samples treated with Fe_3O_4 NPs, e.g., the values of T_B , H_c , M_r at 10 K, and M_s at 300 K were found to exhibit a similar trend as observed in the data obtained in roots (see Table 2).

Our findings indicate that various organs of common bean plants, cultivated in soil with Fe_3O_4 NPs

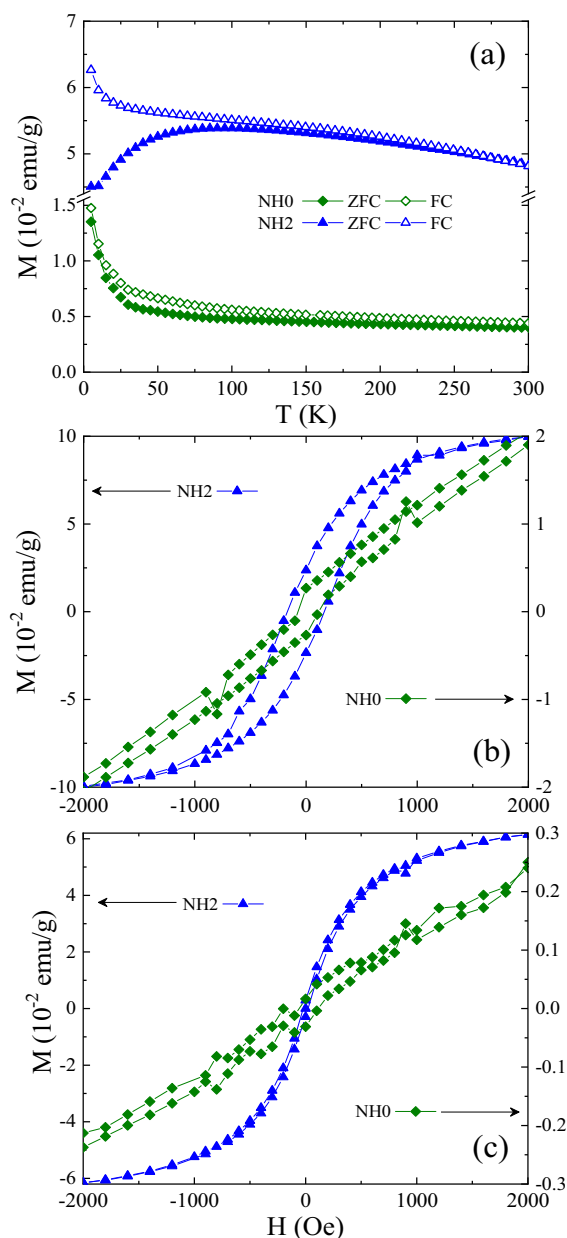


Fig. 6 **a** Temperature dependence $M(T)$ of magnetization curves taken under ZFC (closed symbols) and FC (opened symbols) conditions in nodules samples NH0 and NH2 (Sample labels are listed in Table 1). **b** $M(H)$ curves measured at $T = 10 \text{ K}$. **c** $M(H)$ curves taken at $T = 300 \text{ K}$

and a combination of Fe_3O_4 NPs + *Rhizobium*, can accumulate NPs absorbed from the soil. The occurrence of Fe_3O_4 NPs in roots, nodules, stems, and leaves has been carefully inferred from the similarities seen in the magnetic characterizations ($M(T, H)$

curves) across different plant organs. We emphasize that the measured magnetic signals in plant organs may not exclusively derive from stoichiometric Fe_3O_4 NPs, as has been discussed in our earlier study [24]. We might consider that the chemical instability of small magnetite NPs, when exposed to air and/or water, may experience a partial or even a superficial oxidation, leading to the formation of Fe_3O_4 NPs by exhibiting a magnetite (core)–maghemite $\gamma\text{-Fe}_3\text{O}_4$ (shell) morphology [21] which, in turn, would modify the magnetic volume contribution in a given sample. We also mention that the blocking temperature ($T_B \propto d^3$) was found to be comprehended in a narrow temperature range, roughly from 90 to 105 K (see Table 2), suggesting the occurrence of an eventual maghemite shell width during the process of absorption, translocation, and accumulation of Fe_3O_4 NPs by plant organs.

The increase of the iron content in nodules, roots, and shoots due to magnetite NPs (Fe_3O_4 NPs and *Rhizobium* + Fe_3O_4 NPs treatments) indicates that magnetite NPs induce a greater ability of the plant to extract iron-based compounds from the soil. This could potentially result in an enhancement of both iron mobilization in the rhizosphere and the uptake rate of iron or Fe_3O_4 NPs, supplying enough iron to nodules, roots, and shoots to increase their iron content. Notably, nodules had been observed to have higher iron concentrations than roots and shoots. Moreover, the internal iron concentration required for maximal nodule mass is much higher than that for host roots, implying that nodule formation may require higher internal iron concentration than host growth [15]. This need for iron within the symbiosis is emphasized by the proportion of iron within the nodules compared to other plant organs. Approximately 24% of the soluble iron within the nodule is found in leghemoglobin [46]. Consequently, iron assumes a crucial role in sustaining the nodule environment for symbiosis. Considering the significance of iron symbiosis to sustainable agriculture, it becomes imperative to attain a comprehensive understanding of the intricate processes underlying iron acquisition, storage, and mobilization. During the developmental stages of nodules, there are dynamic variations in the concentration and distribution of iron within the nodule, corresponding the evolving role of the symbiotic organ over time. Some results of interest on this subject were obtained by

synchrotron-based X-ray fluorescence to monitor the iron distribution in indeterminate *M. truncatula* nodules. The results, reported by [57], supported the previously proposed theories concerning the movement of iron within the nodule.

It is noteworthy to emphasize that the occurrence of iron in nodules is closely related to the use of Fe_3O_4 NPs in treatments comprised of Fe_3O_4 NPs and the combined treatment of Fe_3O_4 NPs and *Rhizobium*. Consequently, the presence of iron is responsible for inducing a greater nodulation and nitrogen fixation specifically when Fe_3O_4 NPs act synergistically with the *Rhizobium*. The net result of such a combined action in a synergistic way results in an increase in plant growth and dry matter production as well as a higher concentration of Fe, Mn, P, Ca, and K in roots, stems, and leaves [14]. This phenomenon could be attributed, in principle, to the ability of Fe_3O_4 -NPs to activate nodule gene expression of *Rhizobium* and thereby enhancing nodule formation and biological nitrogen fixation.

Recent advances in genome sequencing, including integration of transcriptomics, proteomics, and metabolomics, have paved the way for identifying transport functions and are also needed for determining the impact of NPs on plants. In particular, the large-scale sequencing of *M. truncatula*, *Lotus japonicus*, and *G. max* genomes have substantially expanded the catalog of genes encoding membrane proteins [7], with a significant number being highly expressed in nodules, some of which are presumed to be iron transporters. The challenge lies in functionally characterizing these transporters and elucidating their location and roles within nodules. A very interesting aspect, considering the mobility, reactivity, biological availability, or potential toxicity of NPs, involves a deeper understanding of their interactions, where the chemistry of colloids is also a contributing factor. Additionally, nanoparticle science methods should be combined with quantum physics rather than focus entirely on classical physics to explain the mechanics of soil and plant physiology improvement.

Conclusions

We successfully investigated the impact of Fe_3O_4 nanoparticles and *Rhizobium* inoculation on the nodulation and growth of common bean plants.

The application of Fe_3O_4 NPs, alone or combined with *Rhizobium* inoculation, resulted in a significant increase in the iron content within plant organs. This increase indicates the absorption, translocation, and accumulation of Fe_3O_4 NPs throughout different parts of the plants. These treatments also led to an enhanced number of nodules per plant, increased active nodules, and greater nodule dry weight. This enhancement contributed to improved symbiotic nitrogen fixation, as evidenced by the increased total nitrogen content in both shoots and roots. Furthermore, our temperature and magnetic field dependence of magnetization ($M(T, H)$) data indicated a progressive and systematic decrease in the magnetization signal in roots, nodules, stems, and leaves of plants treated with Fe_3O_4 NPs, alone or combined with *Rhizobium*. By analyzing magnetic parameters such as blocking temperature, saturation magnetization, coercive field, and remanent magnetization, we concluded that Fe_3O_4 NPs are taken up by the roots, transported throughout the plant, and accumulated in the aerial organs of common bean plants. Additionally, similarities in magnetic properties extracted from different plant parts confirmed that Fe_3O_4 NPs were responsible for the observed magnetic signals across a wide range of temperatures and applied magnetic fields. Our findings demonstrate that a large number of Fe_3O_4 NPs in the soil can be absorbed by the roots, translocated to aerial parts, and accumulated in nodules, stems, and leaves. This accumulation enhances the symbiotic performance between *Rhizobium* leguminosarum (CF1 strain) and common bean plants, promoting nodulation and nitrogen fixation.

Acknowledgements The authors acknowledge the financial support provided by the Brazil's agencies Fundação de Amparo à Pesquisa do Estado de São Paulo (FAPESP) (Grant Nos. 2014/12392-3, 2014/19245-6, and 2013/07296-2) and Conselho Nacional de Desenvolvimento Científico e Tecnológico (CNPq) (Grant Nos. 168255/2014-6, 444712/2014-3, 501446/2014-1, 308706/2007-2, 301463/2019-0, and 304614/2023-8). The authors would thank and to dedicate this article to the memory of Prof. Ben Greenebaum, University of Wisconsin-Parkside, and Prof. J. Derek Bewley, University of Guelph, for their valuable comments and suggestions on the manuscript that allowed us to achieving success in the investigation.

Author contributions E. G-A: wrote de main manuscript, experiment, conceptualization, methodology, Data curation, Analysis A. DS.: wrote first version, plant growth, data curation, figure creation, conceptualization E. G-P: Plant growth, methodology, manuscript correction, S. H. M.: Data curation,

wrote and corrected the manuscript, magnetic measurements F. B. E. L. M. R.: Nanoparticle synthesis & characterization L. M. R.: Nanoparticle synthesis & characterization, Funding R. L.-S.: Plant growth & funding, conceptualization R. F. J.: Magnetic measurements, manuscript correction, methodology, funding.

Data availability No datasets were generated or analysed during the current study.

Declarations

Competing interests The authors declare no competing interests.

References

- Alimi OS, Farner Budarz J, Hernandez LM, Tufenkji N (2018) Microplastics and nanoplastics in aquatic environments: aggregation, deposition, and enhanced contaminant transport. *Environ Sci Technol* 52:1704–1724
- Allito BB, Ewusi-Mensah N, Logah V (2020) Legume-Rhizobium strain specificity enhances nutrition and nitrogen fixation in Faba Bean (*Vicia faba* L.). *Agronomy* 10:826
- Awal Sembada A, Lenggono IW (2024) Transport of nanoparticles into plants and their detection methods. *Nanomaterials* 14(2):131. <https://doi.org/10.3390/nano14020131>
- Azizi-Lalabadi M, Ehsani A, Divband B, Alizadeh-Sani M (2019) Antimicrobial activity of Titanium dioxide and Zinc oxide nanoparticles supported in 4A zeolite and evaluation the morphological characteristic. *Sci Rep* 9(1):Article 1. <https://doi.org/10.1038/s41598-019-54025-0>
- Becana M, Klucas RV (1992) Oxidation and reduction of leghemoglobin in root nodules of leguminous plants. *Plant Physiol* 98(4):1217–1221
- Ben-Moshe T, Frenk S, Dror I, Minz D, Berkowitz B (2013) Effects of metal oxide nanoparticles on soil properties. *Chemosphere* 90(2):640–646. <https://doi.org/10.1016/j.chemosphere.2012.09.018>
- Benedito VA, Li H, Dai X, Wandrey M, He J, Kaundal R, Torres-Jerez I, Gomez SK, Harrison MJ, Tang Y, Zhao PX, Udvardi MK (2010) Genomic inventory and transcriptional analysis of medicago truncatula transporters. *Plant Physiol* 152(3):1716–1730. <https://doi.org/10.1104/pp.109.148684>
- Berrada H, Fikri-Benbrahim K (2014) Taxonomy of the rhizobia: current perspectives. *Br Microbiol Res J* 4:616–639
- Brear EM, Day DA, Smith PM (2013) Iron: an essential micronutrient for the legume-rhizobium symbiosis. *Front Plant Sci* 4:359
- Chen H (2018) Metal based nanoparticles in agricultural system: behavior, transport, and interaction with plants. *Chem Speciat Bioavail* 30(1):123–134
- Dakora FD (1995) A functional relationship between leghaemoglobin and nitrogenase based on novel measurements of the two proteins in legume root nodules. *Ann Bot* 75(1):49–54
- Day DA, Smith PMC (2021) Iron transport across symbiotic membranes of nitrogen-fixing legumes. *Int J Mol Sci* 22(1):432
- Deaker R, Roughley RJ, Kennedy IR (2004) Legume seed inoculation technology—a review. *Soil Biol Biochem* 36:1275–1288
- De Souza A, Govea-Alcaide E, Masunaga SH, Fajardo-Rosabal L, Effenberger F, Rossi LM, Jardim RF (2019) Impact of Fe₃O₄ nanoparticle on nutrient accumulation in common bean plants grown in soil. *SN Appl Sci* 1(4):308. <https://doi.org/10.1007/s42452-019-0321-y>
- De Souza-Torres A, Govea-Alcaide E, Gómez-Padilla E, Masunaga SH, Effenberger FB, Rossi LM, López-Sánchez R, Jardim RF (2021) Fe₃O₄ nanoparticles and *Rhizobium* inoculation enhance nodulation, nitrogen fixation and growth of common bean plants grown in soil. *Rhizosphere* 17:100275. <https://doi.org/10.1016/j.rhisph.2020.100275>
- Dizaj SM, Lotfipour F, Barzegar-Jalali M, Zarrintan MH, Adibkia K (2014) Antimicrobial activity of the metals and metal oxide nanoparticles. *Mater Sci Eng C* 44:278–284
- Dupont L, Alloing G, Pierre O, El Msehli S, Hopkins J, Hérouart D, Frendo P (2012) The legume root nodule: from symbiotic nitrogen fixation to senescence. In: Nagata T (ed) *Senescence*. Intech Publisher, pp 137–157
- El-Temsah YS, Oughton DH, Joner EJ (2013) Effects of nano-sized zero-valent iron on DDT degradation and residual toxicity in soil: a column experiment. *Plant Soil* 368(1):189–200. <https://doi.org/10.1007/s11104-012-1509-8>
- Ercan I, Tombuloglu H, Alqahtani N, Alotaibi B, Bamhrez M, Alshumrani R, Ozelik S, Kaye TS (2022) Magnetic field effects on the magnetic properties, germination, chlorophyll fluorescence, and nutrient content of barley (*Hordeum vulgare* L.). *Plant Physiol Biochem* 170:36–48. <https://doi.org/10.1016/j.plaphy.2021.11.033>
- Fatima Z, Zia M, Chaudhary MF (2007) Interactive effect of *Rhizobium* strains and P on soybean yield, nitrogen fixation and soil fertility. *Pak J Bot* 39(1):255. <https://pdfs.semanticscholar.org/f50b/f08c72941791724fd384eb9a58e34024467e.pdf>
- Frison R, Cernuto G, Cervellino A, Zaharko O, Colonna GM, Guagliardi A, Masciocchi N (2013) Magnetite-maghemite nanoparticles in the 5–15 nm range: correlating the core-shell composition and the surface structure to the magnetic properties. A total scattering study. *Chem Mater* 25(23):4820–4827. <https://doi.org/10.1021/cm403360f>
- Ghafariyan MH, Malakouti MJ, Dadpour MR, Stroeve P, Mahmoudi M (2013) Effects of magnetite nanoparticles on soybean chlorophyll. *Environ Sci Technol* 47:1645–1662
- Ghrir AM, Ingwersen J, Streck T (2010) Immobilization of heavy metals in soils amended by nanoparticulate zeolitic tuff: sorption-desorption of cadmium. *J Plant Nutr Soil Sci* 173(6):852–860. <https://doi.org/10.1002/jpln.200900053>
- Govea-Alcaide E, Masunaga SH, De Souza A, Fajardo-Rosabal L, Effenberger FB, Rossi LM, Jardim RF (2016) Tracking iron oxide nanoparticles in plant organs using magnetic measurements. *J Nanopart Res* 18(10):305. <https://doi.org/10.1007/s11051-016-3610-z>

25. González-Melendi P, Fernández-Pacheco R, Coronado MJ, Corredor E, Testillano PS, Risueño MC, Marquina C, Ibarra MR, Rubiales D, Pérez-de-Luque A (2008) Nanoparticles as smart treatment-delivery systems in plants: assessment of different techniques of microscopy for their visualization in plant tissues. *Ann Bot* 101:187–195
26. Grillo R, Mattos BD, Antunes DR, Forini MML, Monikh FA, Rojas OJ (2021) Foliage adhesion and interactions with particulate delivery systems for plant nanobionics and intelligent agriculture. *Nano Today* 37:101078
27. Guerinot ML (1991) Iron uptake and metabolism in the Rhizobia legume symbioses. *Plant Soil* 130:199–209
28. Hardarson G, Atkins C (2003) Optimizing biological N₂ fixation by legumes in farming systems. *Plant Soil* 252:41–54
29. Havlin JE, Beaton JD, Nelson WL, Tisdal SL (1999) Soil fertility and fertilizers. An introduction to soil management, 6th edn. Prentice Hall, Inc., p 634
30. Hong J, Wang C, Wagner DC, Gardea-Torresdey JL, He F, Rico CM (2021) Foliar application of nanoparticles: mechanisms of absorption, transfer, and multiple impacts. *Environ Sci Nano* 8(5):1196–1210. <https://doi.org/10.1039/D0EN01129K>
31. Iannone MF, Groppa MD, de Sousa ME, Fernández van Raap MB, Benavides MP (2016) Impact of magnetite iron oxide nanoparticles on wheat (*Triticum aestivum* L.) development: evaluation of oxidative damage. *Environ Exp Bot* 131:77–88
32. Jampilek J, Kráľová K (2017) Nanomaterials for delivery of nutrients and growth-promoting compounds to plants. In Prasad R, Kumar M, Kumar V (eds) *Nanotechnology: an Agricultural Paradigm*. Springer Singapore, pp 177–226. https://doi.org/10.1007/978-981-10-4573-8_9
33. Jiang Y, MacLean DE, Perry GE, Marsolais F, Hill B, Pauls KP (2020) Evaluation of beneficial and inhibitory effects of nitrate on nodulation and nitrogen fixation in common bean (*Phaseolus vulgaris*). *Legume Sci* e45:1–11
34. Jo Y-K, Kim BH, Jung G (2009) Antifungal activity of silver ions and nanoparticles on phytopathogenic fungi. *Plant Dis* 93(10):1037–1043. <https://doi.org/10.1094/PDIS-93-10-1037>
35. Khan I, Saeed K, Khan I (2019) Nanoparticles: properties, applications and toxicities. *Arab J Chem* 12:908–931
36. Khan I, Awan SA, Rizwan M, Hassan ZU, Akram MA, Tariq R, Brestic M, Xie W (2022) Nanoparticle's uptake and translocation mechanisms in plants via seed priming, foliar treatment, and root exposure: a review. *Environ Sci Pollut Res* 29:89823–89833
37. Khater MS (2015) Magnetite-nanoparticles effects on growth and essential oil of peppermint. *Curr Sci Int* 4(2):140–144
38. Khot LR, Sankaran S, Maja JM, Ehsani R, Schuster EW (2012) Applications of nanomaterials in agricultural production and crop protection: a review. *Crop Prot* 35:64–70. <https://doi.org/10.1016/j.cropro.2012.01.007>
39. Kim SA, Guerinot ML (2007) Mining iron: iron uptake and transport in plants. *FEBS Lett* 581:2273–3228
40. Kurapov YA, Vazhnichaya EM, Litvin SM, Romanenko SM, Didikin GG (2019) Physical synthesis of iron oxide nanoparticles and their biological activity in vivo. *SN Appl Sci* 1:102
41. Laeremans T, Vanderleyden J (1998) Review: infection and nodulation signalling in Rhizobium-Phaseolus vulgaris symbiosis. *World J Microbiol Biotechnol* 14:787–808
42. Laurent S, Forge D, Port M, Roch A, Robic C, Vander Elst L, Muller RN (2008) Magnetic iron oxide nanoparticles: synthesis, stabilization, vectorization, physicochemical characterizations, and biological applications. *Chem Rev* 108:2064–2110
43. Lin S, Reppert J, Hu Q, Hudson JS, Reid ML, Ratnikova TA, Rao AM, Luo H, Ke PC (2009) Uptake, translocation, and transmission of carbon nanomaterials in rice plants. *Small* 5:1128–1132
44. Ling D, Hyeon T (2013) Chemical design of biocompatible iron oxide nanoparticles for medical applications. *Small* 9:1450–1466
45. Linlin Wang CH, Shao L (2017) The antimicrobial activity of nanoparticles: present situation and prospects for the future. *Int J Nanomed* 12:1227–1249. <https://doi.org/10.2147/IJN.S121956>
46. Lindström K, Mousavi SA (2019) Effectiveness of nitrogen fixation in rhizobia. *Microb Biotechnol* 13:1–22
47. MalekiDizaj S, Mennati A, Jafari S, Khezri K, Adibkia K (2015) Antimicrobial activity of carbon-based nanoparticles. *Adv Pharm Bull* 5(1):19–23. <https://doi.org/10.5681/apb.2015.003>
48. Movchan BA, Kurapov YuA, Didikin GG, Litvin SG, Romanenko SM (2011) Control of the composition and structure of Fe-O nanoparticles during Fe₃O₄ electron beam evaporation. *Powder Metall Met Ceram* 50(3–4):167–172
49. Mutch LA, Tamimi SM, Young JPW (2003) Genotypic characterization of rhizobia nodulating Vicia faba from the soils of Jordan: a comparison with UK isolates. *Soil Biol Biochem* 35:709–714
50. Nguyen MD, Tran H-V, Xu S, Lee TR (2021) Fe₃O₄ nanoparticles: structures, synthesis, magnetic properties, surface functionalization, and emerging applications. *Appl Sci* 11:11301
51. Peoples MB, Herridge DF, Ladha JK (1995) Biological nitrogen fixation: an efficient source of nitrogen for sustainable agricultural production. *Plant Soil* 174:3–28
52. Prevost D, Bromfield ESP (2003) Diversity of symbiotic rhizobia resident in Canadian soils. *Can J Plant Sci* 83:311–319
53. Racuciu M, Creangă DE (2007) Influence of water-based ferrofluid upon chlorophylls in cereals. *J Magn Mater* 311:291–294
54. Reinprecht Y, Schram L, Marsolais F, Smith TH, Hill B, Pauls KP (2020) Effects of nitrogen application on nitrogen fixation in common bean production. *Front Plant Sci* 11:1172
55. Rico CM, Majumdar S, Duarte-Gardea M, Peralta-Videa JR, Gardea-Torresdey JL (2011) Interaction of nanoparticles with edible plants and their possible implications in the food chain. *J Agric Food Chem* 59:3485–3498
56. Rossi LM, Vono LL, Silva FP, Kiyohara PK, Duarte EL, Matos JR (2007) A magnetically recoverable scavenger for palladium based on thiol-modified magnetite nanoparticles. *Appl Catal A* 330:139–144
57. Rodríguez-Haas B, Finney L, Vogt S, González-Melendi P, Imperial J, González-Guerrero M (2013) Iron

- distribution through the developmental stages of *Medicago truncatula* nodules. *Metallomics* 5(9):1247–1253. <https://doi.org/10.1039/c3mt00060e>
58. Sessitsch A, Howieson JG, Perret X, Antoun H, Martínez-Romero E (2002) Advances in Rhizobium research. *Crit Rev Plant Sci* 21:323–378
 59. Shakoor N, Jiangcui GD, Azeem K, Ishfaq M, Shakoor A, Ayaz M, Xu M, Rui Y (2021) Uptake and accumulation of nano/microplastics in plants: a critical review. *Nanomaterials* 11(11):2935. <https://doi.org/10.3390/nano11112935>
 60. Siddiqui MH, Al-Whaibi MH, Firoz M, Al-Khaishany MY (2015) Role of Nanoparticles in Plants. In Siddiqui MH, Al-Whaibi MH, Mohammad F (eds) *Nanotechnology and plant sciences: nanoparticles and their impact on plants*. Springer International Publishing, pp 19–35. https://doi.org/10.1007/978-3-319-14502-0_2
 61. Stephens JHG, Rask HM (2000) Inoculant production and formulation. *Field Crops Res* 65:249–258
 62. Tallarida RJ, Murray RB (1987) Newman-Keuls test. In: *Manual of pharmacologic calculations: with computer programs*. Springer New York, pp 121–124. https://doi.org/10.1007/978-1-4612-4974-0_37
 63. Taylor AF, Rylott EL, Anderson CWN, Bruce NC (2014) Investigating the toxicity, uptake, nanoparticle formation and genetic response of plants to gold. *PLoS ONE* 9:e93793
 64. Teja AS, Koh PY (2009) Synthesis, properties, and applications of magnetic iron oxide nanoparticles. *Prog Cryst Growth Charact Mater* 55:22–45
 65. Tombuloglu H, Slimani Y, Tombuloglu G, Almessiere M, Baykal A (2019) Uptake and translocation of magnetite (Fe₃O₄) nanoparticles and its impact on photosynthetic genes in barley (*Hordeum vulgare* L.). *Chemosphere* 226:110–122. <https://doi.org/10.1016/j.chemosphere.2019.03.075>
 66. Tombuloglu H, Slimani Y, Tombuloglu G et al (2020) Engineered magnetic nanoparticles enhance chlorophyll content and growth of barley through the induction of photosystem genes. *Environ Sci Pollut Res* 27:34311–34321. <https://doi.org/10.1007/s11356-020-09693-1>
 67. Tombuloglu H, Albenayyan N, Slimani Y et al (2022a) Fate and impact of maghemite (γ -Fe₂O₃) and magnetite (Fe₃O₄) nanoparticles in barley (*Hordeum vulgare* L.). *Environ Sci Pollut Res* 29:4710–4721. <https://doi.org/10.1007/s11356-021-15965-1>
 68. Tombuloglu H, Slimani Y, Akhtar S, Alsaheed M, Tombuloglu G, Almessiere MA, Toprak MS, Sozeri H, Baykal A, Ercan I (2022b) The size of iron oxide nanoparticles determines their translocation and effects on iron and mineral nutrition of pumpkin (*Cucurbita maxima* L.). *J Magn Magn Mater* 564, Part 1:170058. <https://doi.org/10.1016/j.jmmm.2022.170058>
 69. Ullah S, Adeel M, Zain M, Rizwan M, Irshad MK, Jilani G, Hameed A, Khan A, Arshad M, Raza A, Baluch MA, Rui Y (2020) Physiological and biochemical response of wheat (*Triticum aestivum*) to TiO₂ nanoparticles in phosphorous amended soil: a full life cycle study. *J Environ Manage* 263:110365. <https://doi.org/10.1016/j.jenvman.2020.110365>
 70. Unkovich M, Herridge D, Peoples M, Cadisch G, Boddey B, Giller K, Alves B, Chalk P et al (2008) Measuring plant-associated nitrogen fixation in agricultural systems. Australian Centre for International Agricultural Research (ACIAR), Bruce
 71. Vincent JM (1970) *Manual for the practical study of root-nodule bacteria*. I.B.P.15. Handbook No 15. Blackwell Scientific Publications, Oxford
 72. Wang X, Xie H, Wang P, Yin H (2023) Nanoparticles in plants: uptake, transport and physiological activity in leaf and root. *Materials* 16(8). <https://doi.org/10.3390/ma16083097>
 73. Wilker J, Navabi A, Rajcan I, Marsolais F, Hill B, Torkamaneh D, Pauls KP (2019) Agronomic performance and nitrogen fixation of heirloom and conventional dry bean varieties under low-nitrogen field conditions. *Front Plant Sci* 10:952
 74. Wohlmuth J, Tekielska D, Čechová J, Baránek M (2022) Interaction of the nanoparticles and plants in selective growth stages—usual effects and resulting impact on usage perspectives. *Plants* 11(18). <https://doi.org/10.3390/plants11182405>
 75. Yandell B (2017) *Practical data analysis for designed experiments*. Routledge. <https://doi.org/10.1016/j.jmsec.2014.08.031>
 76. Zhang Y, Liu N, Wang W, Sun J, Zhu L (2020) Photosynthesis and related metabolic mechanism of promoted rice (*Oryza sativa* L.) growth by TiO₂ nanoparticles. *Front Environ Sci Eng* 14(6):103. <https://doi.org/10.1007/s11783-020-1282-5>
 77. Zhu H, Han J, Xiao JQ, Jin Y (2008) Uptake, translocation, and accumulation of manufactured iron oxide nanoparticles by pumpkin plants. *J Environ Monit* 10(6):713–717. <https://doi.org/10.1039/B805998E>

Publisher's Note Springer Nature remains neutral with regard to jurisdictional claims in published maps and institutional affiliations.

Springer Nature or its licensor (e.g. a society or other partner) holds exclusive rights to this article under a publishing agreement with the author(s) or other rightsholder(s); author self-archiving of the accepted manuscript version of this article is solely governed by the terms of such publishing agreement and applicable law.